Diffraction of evanescent waves and nanomechanical displacement detection

Devrez M. Karabacak,[1] Kamil L. Ekinci,[1] Choon How Gan,[2] Gregory J. Gbur,[2] M. Selim Ünlü,[3] Stephen B. Ippolito,[3,6] Bennett B. Goldberg,[4] and P. Scott Carney[5,*]

[1]*Department of Aerospace and Mechanical Engineering, Boston University, Boston, Massachusetts 02215, USA*
[2]*Department of Physics and Optical Science, University of North Carolina Charlotte, Charlotte, North Carolina 28223, USA*
[3]*Department of Electrical and Computer Engineering, Boston University, Boston, Massachusetts 02215, USA*
[4]*Department of Physics, Boston University, Boston, Massachusetts 02215, USA*
[5]*Department of Electrical and Computer Engineering and The Beckman Institute for Advanced Science and Technology, University of Illinois at Urbana-Champaign, Urbana, Illinois 61801, USA*
[6]*Present address: IBM T. J. Watson Research Center, 1101 Kitchawan Road, 11–141, Yorktown Heights, New York 10598, USA*
[*]*Corresponding author: carney@uiuc.edu*

Received January 2, 2007; revised March 23, 2007; accepted April 4, 2007; posted April 27, 2007 (Doc. ID 78603); published June 21, 2007

Sensitive displacement detection has emerged as a significant technological challenge in mechanical resonators with nanometer-scale dimensions. A novel nanomechanical displacement detection scheme based upon the scattering of focused evanescent fields is proposed. The sensitivity of the proposed approach is studied using diffraction theory of evanescent waves. Diffraction theory results are compared with numerical simulations. © 2007 Optical Society of America

OCIS codes: 050.1960, 120.7280.

Nanometer-scale mechanical resonators and nanoelectromechanical systems (NEMS) are being developed for a number of sensing, computing, and signal processing applications. These promising devices have tiny masses, low intrinsic dissipation, and high fundamental resonance frequencies, resulting in unprecedented accuracy and sensitivity in the aforementioned applications [1,2]. However, detection at the nanoscale remains a challenge, hindering efforts to achieve the full potential of NEMS.

Optical techniques are useful in displacement detection because they are sensitive, broadband, and nondestructive [3,4]. However, the displacement of the structure under study must significantly change the scattered optical field for a sensitive measurement and dynamic scattering from a moving subwavelength structure, such as a nanomechanical resonator, is usually weak compared with the static background signal. For sensitive detection, the incident field must be well localized so that scattered signal from the moving nanostructure is maximized. Furthermore, total incident optical power must be reduced to ensure that the technique is indeed nondestructive. To address some of these issues, a dark-field optical technique is proposed here and a novel application of diffraction theory to evanescent waves is used to carry out the analysis. Analytic diffraction theory is compared with numerical simulation.

The geometry of the problem is illustrated in Fig. 1. The suspended nanomechanical resonator is modeled as a thin black strip of infinite length with width w; the resonator (strip) is positioned at a height Δ above the interface of the dielectric substrate half-space. An assumption of infinite length is valid for experimental nanomechanical devices [3], as they usually have a high aspect ratio with length much greater than the diameter of a tightly focused optical spot. The planar dielectric boundary between the substrate and vacuum within the arrangement allows for the generation of a highly localized evanescent field around the structure. An enhanced (focused) evanescent field can be generated with a numerical aperture increasing lens (NAIL) [5], as illustrated in the inset of Fig. 1.

The scattered field is calculated by means of the Kirchhoff diffraction integral [6]. Since the incident field is evanescent and therefore does not propagate, Babinet's principle may be applied with the result that the field diffracted by the strip and propagated to the far zone is identical to the field diffracted by a

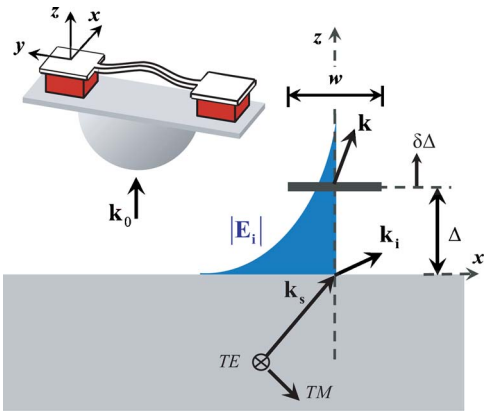

Fig. 1. (Color online) Cross-sectional (x–z plane) view of the proposed detection. Here, an infinitely long strip of width w is suspended by Δ and oscillates with amplitude $\delta\Delta$ above a substrate of refractive index n. The device is illuminated by the evanescent field $\mathbf{E_i}$ in the direction of $\mathbf{k_i}$ formed by the total internal reflection of the incoming wave in the direction of $\mathbf{k_s}$. This scheme can be realized by illuminating a typical doubly clamped nanomechanical resonator through an index-matched NAIL attached to the backside of the sample, as shown in the inset.

slit in a screen placed at the same plane up to an overall sign. The surface of the strip parallel to the interface is denoted by A, and the incident field is denoted by $\mathbf{E}_i$. The resultant diffraction integral for the far-zone field $\mathbf{E}$ is given by the expression

$$\mathbf{E}(\mathbf{r}) = -\frac{1}{4\pi}\int_A \mathrm{d}^2 r'[\mathbf{E}_i(\mathbf{r}') \times \nabla \times G(\mathbf{r},\mathbf{r}') - G(\mathbf{r},\mathbf{r}') \times \nabla \times \mathbf{E}_i(\mathbf{r}')] \cdot \mathbf{n}. \quad (1)$$

Here, G is the half-space dyadic Green function that satisfies the wave equation in the upper and lower half-spaces separately (except at $\mathbf{r}=\mathbf{r}'$) and obeys the boundary conditions that $\mathbf{n}\times G$ and $\mathbf{n}\times\nabla\times G$ are continuous, commensurate with the condition on the tangential components of the electric and magnetic fields [7].

Since only the forward-scattered field is relevant for this problem, the Green dyad is expressed for $z > z'$,

$$G(\mathbf{r},\mathbf{r}') = \frac{i}{2\pi}\int \mathrm{d}^2 k_\parallel e^{i\mathbf{k}\cdot(\mathbf{r}-\mathbf{r}')}\frac{1}{k_z}[D(\mathbf{k}) + e^{2ik_z z'}R(\mathbf{k})], \quad (2)$$

where $\mathbf{k}=(\mathbf{k}_\parallel,k_z)$, $k_z=\sqrt{k_0^2-k_\parallel^2}$, and D and R are the dyadic quantities that ensure the transversality of, respectively, (i) the plane-wave propagated directly from $\mathbf{r}'$ to $\mathbf{r}$ and (ii) the plane-wave propagated via reflection from the interface. The dyads may be written as

$$D(\mathbf{k}) = \hat{u}_{te}(\mathbf{k})\hat{u}_{te}(\mathbf{k}) + \hat{u}_{tm}(\mathbf{k})\hat{u}_{tm}(\mathbf{k}), \quad (3)$$

$$R(\mathbf{k}) = \hat{u}_{te}(\mathbf{k})r_{te}\hat{u}_{te}(\tilde{\mathbf{k}}) + \hat{u}_{tm}(\mathbf{k})r_{tm}\hat{u}_{tm}(\tilde{\mathbf{k}}), \quad (4)$$

where $\hat{u}_{te/tm}$ are the unit vectors of the TE/TM basis relative to $\mathbf{k}$. These unit vectors may be constructed as $\hat{u}_{te}(\mathbf{k})=\mathbf{k}\times\mathbf{n}/|\mathbf{k}\times\mathbf{n}|$ and $\hat{u}_{tm}(\mathbf{k})=\mathbf{k}\times\hat{u}_{te}/|\mathbf{k}\times\hat{u}_{te}|$. Here, $\hat{k}=\hat{u}_{te}\times\hat{u}_{tm}=\mathbf{k}/|\mathbf{k}|$ so that $\hat{k}$, $\hat{u}_{te}$, $\hat{u}_{tm}$ form an ordered orthonormal triple with $\hat{u}_{te}$ always parallel to the interface. The vector $\tilde{\mathbf{k}}$ is defined to be the reflection of $\mathbf{k}$ through the $z=0$ plane, i.e., $\tilde{\mathbf{k}}=(\mathbf{k}_\parallel,-k_z)$. The reflected waves for $\hat{u}_{te/tm}(\tilde{\mathbf{k}})$ can be defined in a similar fashion. The quantities r_{te} and r_{tm} are the respective Fresnel coefficients for TE and TM waves, given by $r_{tm}=(n^2k_z-k_z')/(n^2k_z+k_z')$, $r_{te}=(k_z-k_z')/(k_z+k_z')$, and $k_z'=\sqrt{n^2k_0^2-k_\parallel^2}$.

With the incident evanescent field given by $\mathbf{E}_i(\mathbf{r}) = \mathbf{E}_0 e^{i\mathbf{k}_i\cdot\mathbf{r}}$, the diffracted field given by Eq. (1) becomes

$$E_{te/tm}(\mathbf{r}) = \frac{-ie^{ik_0 r}}{2r}\delta(k_y-k_{iy})\frac{\sin[(k_x-k_{ix})w/2]}{(k_x-k_{ix})/2} \times e^{-i(k_z-k_{iz})\Delta}\mathbf{E}_0 \times [\hat{u}_{te/tm}(\mathbf{k}) \times (\mathbf{k}+\mathbf{k}_i) + e^{2ik_z\Delta}r_{te/tm}\hat{u}_{te/tm}(\tilde{\mathbf{k}}) \times (\tilde{\mathbf{k}}+\mathbf{k}_i)] \cdot \mathbf{n}. \quad (5)$$

Here, $\mathbf{k}\|\mathbf{r}$ and the te/tm subscript indicates either transverse electric or transverse magnetic fields relative to the direction of observation.

To understand the limitations of the diffraction theory, the analytical results of Eq. (5) are compared with numerical solutions of Maxwell's equations. This is accomplished by solution of a domain integral equation for the electric field [8], which is constructed with the use of the electromagnetic Green tensor for the vacuum/substrate system. The equations are solved numerically by matrix inversion operations. The strip is modeled as a silver structure of thickness of 50 nm with complex index of refraction $0.385 + i8.95$ at $\lambda = 1.3$ μm. Simulations were done on a desktop machine, with run times less than 1 h. Stability and convergence were checked by varying the discretization mesh and the contour deformation for analytic integration. The numerical results are shown as dashed curves in Fig. 2. The peak of the pattern for the TE incident field is centered for all results. For the TM case, the left peaks in the analytic and numeric results differ by 2.7° for both heights. The right peaks differ by 8.6° for the $\Delta = 100$ nm case and 12° for the $\Delta = 200$ nm case.

In simulation of scattering from wider strips (500 nm) the numerical results and diffraction theory differ considerably for TM-polarized incident fields.

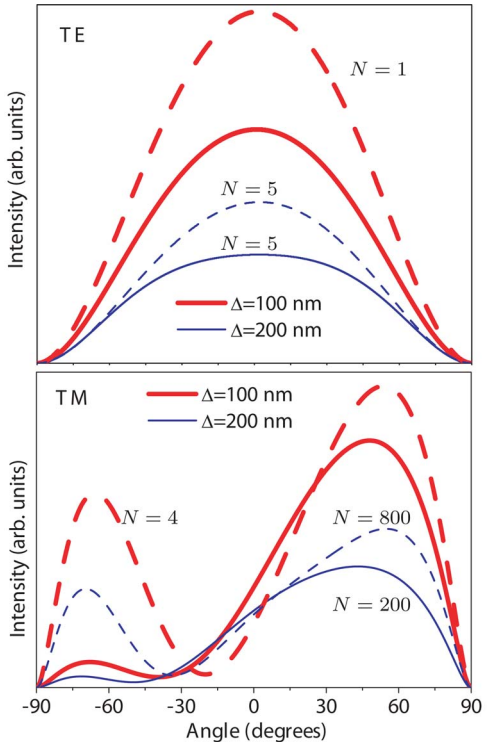

Fig. 2. (Color online) Normalized distribution of the intensity (the squared magnitude of the electric field) as a function of angle in the plane normal to the longitudinal axis of the strip of width $w = 50$ nm. The plots are for different strip heights as indicated. The incident field in vacuum is taken to be of unit amplitude at the Si interface with wavelength $\lambda = 1.3$ μm and a wave vector of $(2.2k_0, 0, 2.0ik_0)$. The dashed curves indicate the results of numerical simulation, and the solid curves the outcome of Eq. (5). In the top panel the incident field is TE-polarized, and in the bottom panel it is TM-polarized. The curves were normalized to the peak height of the analytic result at 100 nm and then scaled by a factor N indicated by the curve for display purposes.

This may occur for the wider strip because the strip–substrate system forms a resonant cavity for the TM-polarized case but not the TE-polarized case. Multiple scattering in this cavity tends to randomize the transverse momentum of the field, moving the peak of the intensity to the middle of the angular range. Use of the diffraction theory should be avoided for such resonant structures.

Finally, a dark-field technique for monitoring nanomechanical resonators is analyzed. That is, by making use of a focused evanescent field, the strip is illuminated such that in the absence of the strip no signal is transmitted to the detector. The optical displacement signal is presented as a function of effective device size w [4]. The fluctuation in the scattered power is calculated as the strip vibrates in the z direction with a conservative amplitude of $\delta\Delta = 0.5$ nm. For the illuminating field, a coherent superposition of evanescent plane waves is taken to form a focused evanescent spot at the surface of the substrate with a spot size (FWHM) of 250 nm at a wavelength of $\lambda = 1.3$ μm. Such subwavelength spots of diameter $\sim\lambda/2n$, where $n = 3.45$ for silicon, have been demonstrated using a NAIL [5]. The angular spectrum of the scattered wave in the far field is computed using Eq. (5) for each plane-wave component of the illuminating field, and the results are summed coherently. A detection system in the far zone with numerical aperture of NA = 0.7 is assumed, and the power contrast induced by the strip motion above the substrate, i.e., by varying the height to $\Delta \pm \delta\Delta$, is computed. The obtained results, shown in Fig. 3, indicate an optimum strip width w for a given spot diameter, or conversely an optimum spot diameter for a given w. This result may be counterintuitive, since most optical methods used at this length scale display a monotonic improvement in the detected signal as the optical spot diameter is reduced. Two factors contribute to this behavior: (i) wide strips push the scattered field into higher angles beyond the collection angle; (ii) diffraction is dominated by the edges of the strip and a tightly focused field concentrates energy away from the edges. For a crude comparison, assuming lossless transmission between the NAIL and device substrate, at an optical input power of 1 mW and $\Delta = 100$ nm, the obtained dynamic signal amplitude from diffraction of evanescent waves is comparable with or higher than commonly used displacement detection schemes in NEMS [3,9]. The promise of the proposed dark-field technique, however, lies in the fact that the background signal is largely eliminated.

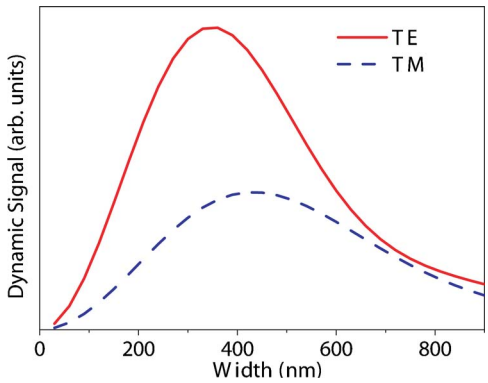

Fig. 3. (Color online) Normalized dynamic signal in the scattered field due to a focus superposition of evanescent waves with a FWHM spot size of 250 nm centered on the strip, at height $\Delta = 100$ nm, due to an oscillation of amplitude $\delta\Delta = 0.5$ nm, for both TE and TM polarization of the incident field.

This work was supported by U.S. Air Force MURI grant F49620-03-1-0379 and NSF NIRT grant 0210752.

References

1. K. L. Ekinci and M. L. Roukes, Rev. Sci. Instrum. **76**, 061101 (2005).
2. H. G. Craighead, Science **290**, 1532 (2000).
3. T. Kouh, D. Karabacak, D. H. Kim, and K. L. Ekinci, Appl. Phys. Lett. **86**, 013106 (2005).
4. D. Karabacak, T. Kouh, C. C. Huang, and K. L. Ekinci, Appl. Phys. Lett. **88**, 193122 (2006).
5. S. B. Ippolito, B. B. Goldberg, and M. S. Ünlü, Appl. Phys. Lett. **78**, 4071 (2001).
6. M. Born and E. Wolf, *Principles of Optics*, 7th ed. (Cambridge U. Press, 1999).
7. P. S. Carney and J. C. Schotland, Opt. Lett. **26**, 1072 (2001).
8. T. D. Visser, H. Blok, and D. Lenstra, IEEE J. Quantum Electron. **35**, 240 (1999).
9. D. Karabacak, T. Kouh, and K. L. Ekinci, J. Appl. Phys. **98**, 124309 (2005).